MDPI

Article

The CYGNO Experiment

Elisabetta Baracchini[1], Luigi Benussi [1] Stefano Bianco [1] Cesidio Capoccia [1] Michele Caponero [1] Gianluca Cavoto [1] André Cortez [1] Igor Abritta Costa [1] Emanuele Di Marco[1] Giulia D'Imperio[1] Giorgio Dho[1] Francesco Iacoangeli[1] Giovanni Maccarrone[1] Michela Marafini[1] Giovanni Mazzitelli[1] Andrea Messina[1] Rafael Antunes Nobrega[1] Emiliano Paoletti[1] Luciano Passamonti[1] Fabrizio Petrucci[1] Davide Piccolo[1] Daniele Pierluigi[1] Davide Pinci[1]* Francesco Renga[1] Filippo Rosatelli[1] Andrea Russo[1] G. Saviano[1] Roberto Tesauro[1] Sandro Tomassini[1]

1 Gran Sasso Science Institute, L'Aquila, I-67100, Italy
2 Istituto Nazionale di Fisica Nucleare, Laboratori Nazionali del Gran Sasso, Assergi, Italy
3 Istituto Nazionale di Fisica Nucleare , Laboratori Nazionali di Frascati, I-00044, Italy
4 ENEA Centro Ricerche Frascati, Frascati, Italy
5 Istituto Nazionale di Fisica Nucleare, Sezione di Roma, I-00185, Italy
6 Dipartimento di Fisica Sapienza Università di Roma, I-00185, Italy
7 Universidade Federal de Juiz de Fora, Juiz de Fora, Brasil
8 Museo Storico della Fisica e Centro Studi e Ricerche "Enrico Fermi", Piazza del Viminale 1, Roma, I-00184, Italy
9 Dipartimento di Matematica e Fisica, Università Roma TRE, Roma, Italy
10 Istituto Nazionale di Fisica Nucleare, Sezione di Roma TRE, Roma, Italy
11 Dipartimento di Ingegneria Chimica, Materiali e Ambiente, Sapienza Università di Roma, Roma, Italy
* Correspondence: davide.pinci@roma1.infn.it
† Current address: Affiliation 3
‡ These authors contributed equally to this work.

Citation: Baracchini E., Benussi L. Bianco S. Capoccia C. Caponero M. Cavoto G. Cortez A. A. Costa I. A. Di Marco E. D'Imperio G. Dho G. Iacoangeli F. Maccarrone G. Marafini M. Mazzitelli G. Messina A. A. Nobrega R. Orlandi A. Paoletti E. Passamonti L. Petrucci F. Piccolo D. Pierluigi D. Pinci D. Renga F. Rosatelli F. Russo A. Saviano G. Tesauro R. Tomassini S. The CYGNO Experiment. *Physics* **2021**, *1*, 1–13. https://doi.org/

Received:
Accepted:
Published:

Abstract: The search for a novel technology able to detect and reconstruct nuclear recoil events in the keVenergy range has become more and more important as long as vast regions of high mass WIMP-like Dark Matter candidate have been excluded. Gaseous Time Projection Chambers (TPC) with optical readout are very promising candidate combining the complete event information provided by TPC technique to the high sensitivity and granularity of last generation scientific light sensors. CYGNO (a CYGNUs module with Optical readout) is an experiment that aims at searching Dark Matter in the low mass region, exploiting very promising performance of the Optical Readout approach of multiple-GEM structures for large volume TPC. This experiment is part the CYGNUS proto-collaboration which aims at constructing a network of underground observatories for directional Dark Matter search. The combined use of high-granularity sCMOS and fast sensors to read out the light allows the reconstruction of the 3D direction of the tracks, offering good energy resolution and very high sensitivity in the keV energy range together with a very good particle identification useful to distinguish nuclear recoils from electronic recoils. A 1 cubic meter demonstrator is expected to be built in 2020/21 aiming to a larger scale apparatus (30m^3-100 m^3), in a later stage.

Keywords: keyword 1; keyword 2; keyword 3 (List three to ten pertinent keywords specific to the article; yet reasonably common within the subject discipline.)

1. Introduction

2. The CYGNO project

The aim of CYGNO project is the development and realisation of a GEM-based Optically Readout Time Projection Chamber for the study of rare events with energy releases in the range 1-100 keV.

As it will be described in this paper, such a technology will allow the study of possible Dark Matter signals in mass regions still un-explored together with the possibility of

A gas represents an interesting target: nuclei free paths can be long enough to be reconstructed. In particular, ϵ the maximum fraction of the energy that can be transferred to the nucleus of mass m_N by a Dark Matter particle of mass m_χ is given by:

$$\epsilon = \frac{4\rho}{(\rho+1)^2} \tag{1}$$

where $\rho = \frac{m_N}{m_\chi}$.

3. The Optical Readout Approach

In recent years different groups started working on the development of optical readout of gas detectors (citazioni). In particular, very interesting results were obtained when CMOS-based sensors were employed for the acquisition of Time Projection Chambers (TPC) equipped with multiplication stages based on Micro-Pattern Gas Detectors (MPDG) (citazioni).

Main limitation in the development of this technique was represented by the low signal/noise ratio of the light sensors. Mainly CCD have being used in past with a noise of 5÷10 photons/pixel. This, allowed to detect only highly ionizing particle tracks.

CYGNO collaboration first proposed the use of CMOS based optical device, for GEM-based detector optical readout [27**? ? ? ?**].

High-granularity and low-noise image sensors in CMOS technology offer high level performance. State-of-the-art imagers contain tens of millions of pixels, with very low dark current (down to 2 e-/s/pixel), sub-electron readout noise and high sensitivity, so that they provide almost single photon detection.

On the other hand, MPDG production technology guarantees very high quality devices, providing stable and uniform operation.

Time projection chambers, developed for high-energy experiment, provide the possible of collecting a complete and useful set of information about events:

- it is possible to make a 3D reconstruction of the tracks in sensitive volume;
- it can evaluate not only the total amount of released energy, but also its profile along the particle trajectory allowing to reconstruct the dE/dx, very helpful for particle identification and track head-tail discrimination;
- large volumes can be acquired with small amount of readout channels.

For equipping large surfaces, the use of Micro Pattern Gas Detectors is a very simple solution ensuring high space and time resolution. In particular Gas Electron Multipliers are able to suppress the Ion Back Flow inside the sensitive volume.

The optical readout approach has several advantages:

- sensors can be installed outside the sensitive volume reducing the interference with the GEM high voltage operation and reducing the gas contamination;
- the use of suitable lenses allows to image large surfaces to small sensors;

3.1. Principle of Operation

Gas luminescence is a well studied and established mechanism: charged particles traveling in the gas can ionize atoms and molecules but can also excite them. During the de-excitation processes, photons are emitted. Amount and spectrum of light produced strongly depends on the gas, on its density and the possible presence and strength of an electric fields [14]. In particular, light production can be induced in the gas by electrons (electro-luminesce) produced in avalanche processes: **during** the multiplication together with secondary electrons or **outside** from multiplication regions [16]. Since the electro-luminesce cross section depends on the electron energy, the different electric field configuration inside and outside the multiplication regions makes the number of photons "produced" by each electron per unit length very different.

3.1.1. The Gas Mixtures

A key role in determining the detector performance is played by the gas mixture characteristics: ionization statistics, transport properties (drift velocity and diffusion), electron multiplication and light production.

Different gas mixtures (Ar/CF_4 and He/CF_4 in different proportions) were studied. The best performance were found for a mixture based on 60% Helium and 40% CF_4 [29]. This mixture is expected to have a broad light emission spectrum with , two main peaks: one around **300 nm** and one around **620 nm** [14].

Simulation of gas mixtures

The parameters of the two gas mixtures relevant to study the electron transport in the field cage were calculated by means of Garfield [31,32]. The behavior of the diffusion coefficients and drift velocity for different electric fields is reported in Fig. 1.

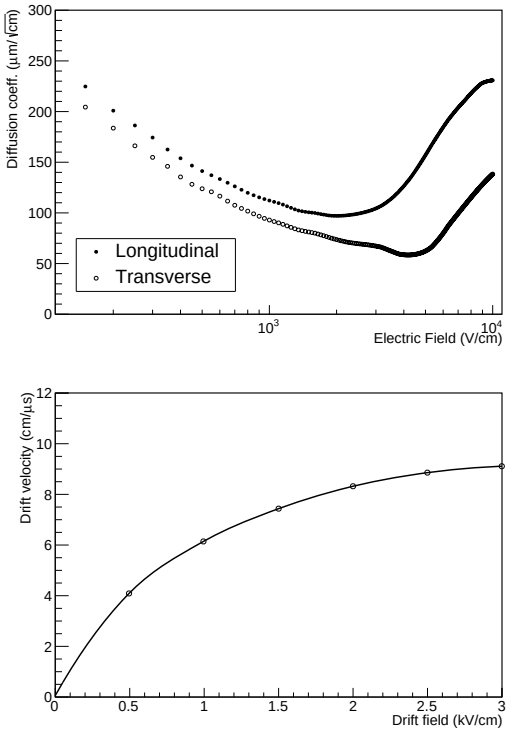

Figure 1. Transverse and longitudinal diffusion coefficients (left) and electron drift velocity (right) as a function of the electric field.

A gas mixture with a large fraction of a "cold gas" as the CF_4 allows to have a small electron diffusion and quite high drift velocities for electric fields below 1 kV/cm.

Effective ranges of electron and He-nuclei recoils were calculated respectively by [33] and SRIM [**?**]. Results as a function of particle kinetic energy are shown in Fig. 2:

- He-nuclei recoils have a sub-millimetre range up to energies of 100 keVand are thus expected to produce bright spots with sizes mainly dominated by diffusion effects;
- low energy (less than 10 keV) electron recoils are in general larger then He-nuclei recoils with same energy and are expected produce less intense spot-like signals. For a kinetic energy of 10 keV, the electron range becomes longer than 1 mm and for few tens of keV, tracks of few centimetres are expected.

Measurements of gas mixture properties

3.1.2. Optical Sensors

In order to perform a 3D track reconstruction, the profile of the electron arrival times on the GEM should be acquired.

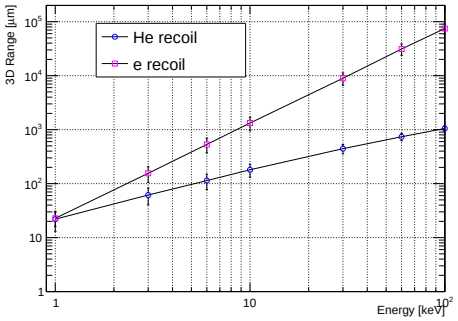

Figure 2. Average projected ranges for electron and He-nuclei recoils as a faction of their kinetic energy.

The main limitation of high granularity CMOS sensors is represented by their poor timing information. The maximum possible readout rate of the order of 1 kHz would not allow to have a "time-stamping" better than 1 ms.

To overcome this limitation, CYGNO collaboration proposed and developed the idea of combining the slow sCMOS camera with fast light sensors (PMT os SiPM). Performance of the combined light readout were tested with the use of a fast PMT [**?**] and it was possible to evaluate a resolution on the reconstructed relative z coordinate of charge clusters of about 100 μm.

sCMOS-based Cameras

As anticipated in Sect.3, high quality cameras are a crucial ingredient for the experiment results. Different cameras were tested during the R&D phases [**?**]. All results shown in the paper were obtained by means of the an ORCA Flash 4.0 camera[1]. This device in based on a 1.33×1.33 cm^2 scientific CMOS sensor, subdivided in 2048×2048 pixels with an active area of 6.5×6.5 μm^2 each, with a quantum efficiency of 70% at 600 nm and a readout noise of 1.4 electrons. The response and noise level of this sensor were tested with a calibrated light source [20]. A response of 0.9 counts/photon was measured together with a pedestal fluctuation of the pedestal of 1.3 photons/pixel.

This sensor was usually equipped with a Schneider lens with 25 mm focal length f and 0.95 aperture a. The lens was placed at the distance d necessary to make the acquisition of the whole GEM surface possible. The geometrical acceptance Ω can be evaluated as [26]:

$$\Omega = \frac{1}{(4(\delta+1) \times a)^2}$$

being $\delta = d/f - 1$ the optical de-magnification.

CYGNO apparatus will be equipped with the latest generation sCMOS-based ORCA-Fusion Digital Camera[2] featuring 2304 *times* 2304 pixels with dimensions of 6.5×6.5 μm^2, providing a quantum efficiency of 80% at 600 nm and a readout noise of 0.7 electrons.

Fast light-sensors

The information provided by a fast light sensor will be exploited to reconstruct the signal time development and, therefore, its projection on the axis orthogonal to the GEM plane. Different PMT and SiPMT were tested during the RD phase to individuate the most appropriate in terms of sensitivity and time resolution.

Results presented here were obtained with a Photonics XP3392 Photo Multiplier Tube (PMT) with a 5 ns rise-time, a maximum QE for 420 nm and a 76 mm square-window.

[1] For more details visit www.hamamatsu.com

[2] https://www.hamamatsu.com/eu/en/product/type/C14440-20UP/index.html

4. Experimental Results

4.1. LEMON*Prototype*

All results reported in this paper were obtained with the Long Elliptical MOdule LEMON. This detector (Fig. 3 is a TPC with a sensitive volume of 7 litres (A) contained in a 20 cm long cylindrical field cage (FC). The base of the cylinder is an ellipse with 24 cm and 20 cm axes. The shape of the FC was chosen in order to couple it with a 24×20 cm^2 triple-GEM stack, that closes the sensitive volume on one side. On the other side, the volume is close be a mesh-based semitransparent cathode. Light produced inside the GEM holes during the multiplication processes is acquired on the GEM side by the ORCA Flash 4.0 camera, and, on the cathode side by the Photonics XP3392 photo-multiplier (Sect. 3.1.2.

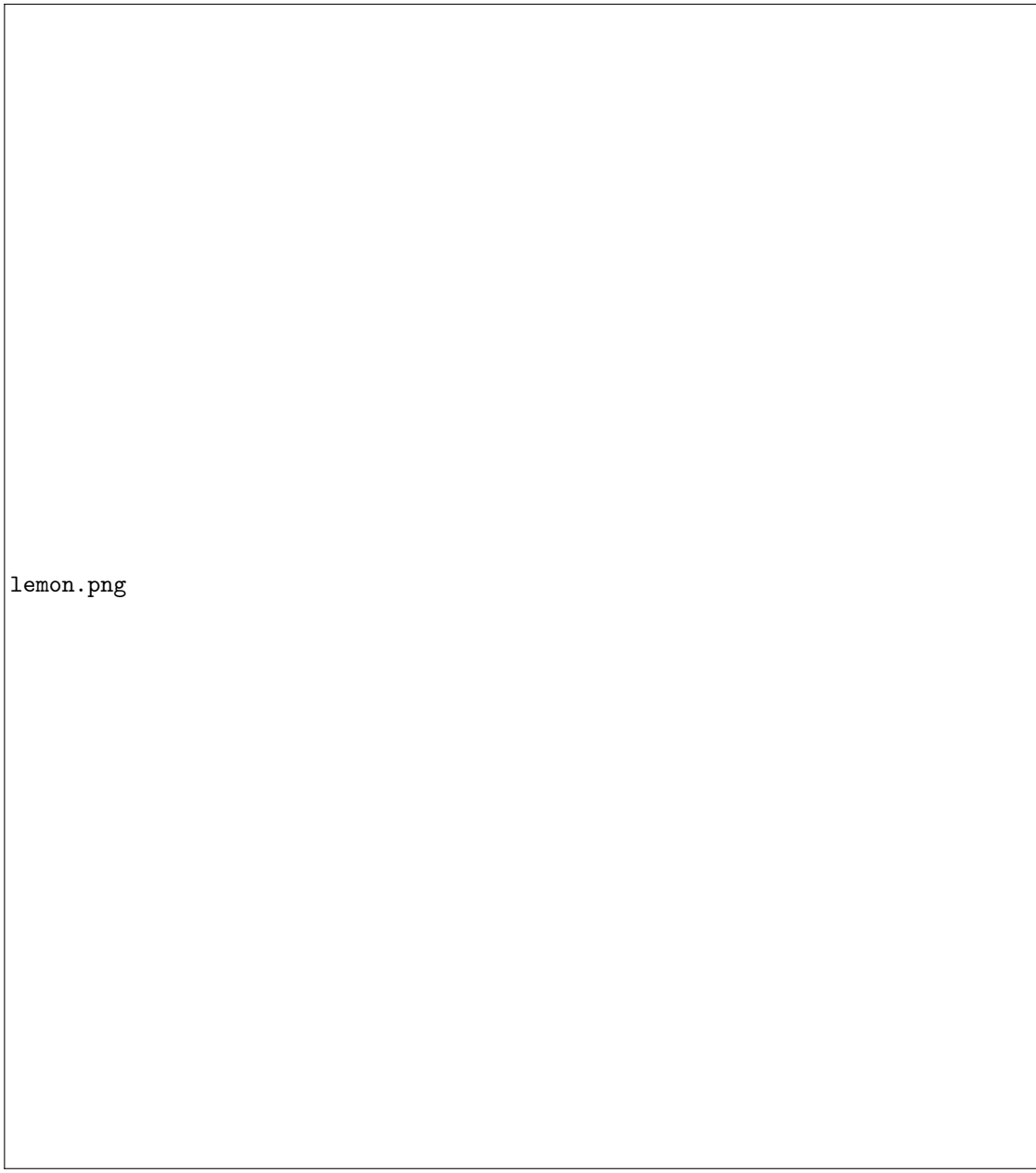

Figure 3. Drawing of the experimental setup. In particular, the elliptical field cage closed on one side by the triple-GEM structure and on the other side by the semitransparent cathode (A), the PMT (B), the adaptable bellow (C) and the CMOS camera with its lens (D) are visible.

The drift volume was filled with He/CF_4 based gas mixtures.

Even if at the beginning they scanned to optimise them, the typical operating configuration for LEMONwas based on following sets:

- a gas flux of 200 cc/min;
- an electric field within the sensitive volume E_D = 0.5 kV/cm;
- an electric field in the 2 mm wide gaps between the GEMs E_{Transf} = 2.5 kV/cm;
- a voltage difference across the two sides of each GEM V_{GEM} = 460 V;

According to results presented in [30], in this configuration an electron gain of about 1.5×10^6 is expected.

4.2. Performance Studies

Performance of LEMONwere tested in recent years in laboratory by means of radioactive sources (^{55}Fe,AmBe), high energy (400 MeV) electrons from a beam at the BTF facility [36,37] and cosmic rays.

4.2.1. Operation Stability

Detector operational stability was evaluated during a month long test [29]. During the whole period the behavior of all currents drawn by the high voltage channels supplying the electrodes of the GEM stack were monitored and recorded. In particular, from the correlated analysis of $I_{G3U}$and images continuously acquired, two different phenomena of electrical instability were observed:

- **Hot spots.** Appearance of tiny luminous spots (less than 1 mm^2 on the GEM surface initially accompanied with a negligible current increase.
  These spots could disappear with time or start to slowly grow up (on a time scale of minutes). At some point they could even involve a currents of the order of tens of nano-amperes.
- **Discharges** High charge density due to very high ionizing particles or charge accumulation on electrode imperfections can suddenly discharge across GEM channels. In these events, a sudden increase in the drawn current is recorded with a voltage restoring on the electrodes through protection resistors on a few seconds time basis. Also these events trigger the recovery procedure. Even if these events are less frequent than hot spots they can be dangerous for the GEM structure and the energy released in the discharge can, in principle, damage it.

A completely automatic high voltage control and recovery procedure was developed. In case of drawn currents larger than a certain threshold all V_{GEM} are decreased of 100 V and then slowly restored in about 3 minutes.

From the monitoring of detector current it resulted an occurrence probability of about 10 hot-spots/day and 6 discharges/day. A detailed analysis of the time distance between two of these phenomena didn't shown any correlation between two subsequent events neither any increase of their rates. This allowed to conclude than detector operation looked very safe and stable and the provided performance was completely satisfactory.

The instability events gave rise to a detection inefficiency due to dead time introduced by recovering procedures of less than 4%.

Other gas proportion were tested and it resulted evident that a lower amount of CF_4, able to quench and avoid large charge productions gave a less stable electrostatic configuration.

4.2.2. Light Yield and Energy Resolution

The light production was evaluated by analysing sCMOS and PMT response for interactions in gas of 5.9 keV produced by a ^{55}Fesource.

Figure 4 shows the spectra of the amount of light detected in spots reconstructed on sCMOS sensor.

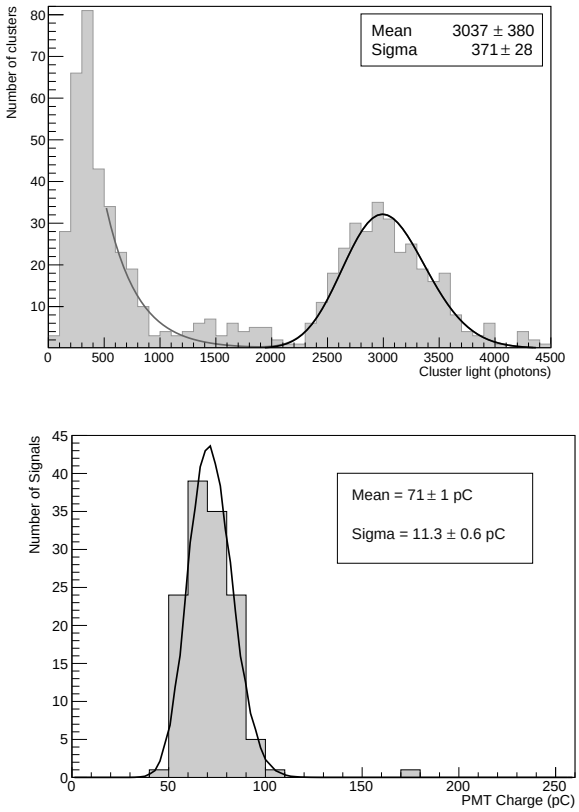

Figure 4. Distribution of the light content in spots (left) and distribution of the charge provided by the PMT (right).

Average light yields for the two mixtures were evaluated from a Polya fit [38] to the two distributions:

- sCSMOS provides an average value of 514 ± 63 detected photons per keV released in the gas (in agreement with results obtained with lower V_{GEM} and E_{Transf} [34]) with an energy resolution of 12.2%;
- PMT provides an average value of (12.0 ± 0.2) pC per keV released in the gas with an energy resolution of 15.5%;

The similar energy resolution provided by the two gas mixture indicates that the main contribution to this parameter is due the fluctuations of electron multiplication processes.

4.2.3. Detection Efficiency

The capability of detecting low energy spots in the sensitive volume was tested by exploiting photons emitted by ^{55}Fesource. Figure 5 shows, on the left, the behavior of the number n of reconstructed spots as a function of electric field in the drift volume normalized to the value obtained for E_D = 600 V/cm. The plateau found for E_D values larger than 300 V/cm indicates that starting from that value, a full detection efficiency is found. On the right of Fig. 5 the behavior of n as a function of spot distance from the GEM plane (right) normalised to its average value $\overline{n}$ is shown.

A constant behavior was found in all tested positions allowing to conclude that no evidences of inefficiency in event detection were found.

4.2.4. Tracking Performance

High energy particles crossing the detector can give rise to tracks several centimetre long. This can be the case for muons from cosmic rays of electron recoils with energies

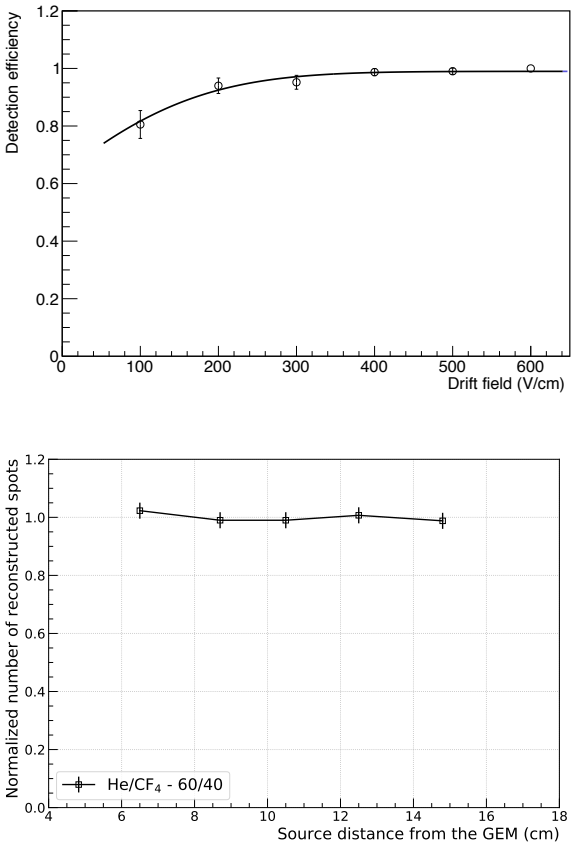

Figure 5. Behavior of the normalized number of ^{55}Fespots as a function of drift electric field (left) and event depth in sensitive volume (right).

of about 100 keV or more. Performance in reconstructing long track were studied at the Beam Test Facility (BTF) of "Laboratori Nazionali di Frascati" [36,37] Reults are described in details in [28**? ?**]. They indicate that track segments with lengths lower than 1 cm can be reconstructed with a resolution on relative position between 100 μm (near the GEM plane) and 300 μm (20 cm far from GEM plane). Moreover, by exploiting the diffusion effect in gas, the distance of each of those segments can be evaluated, separately by the CMOS sensor and PMT, with a precision between 10% and 20%.

5. Detection and Identification of Nuclear Recoils
6. Detection and Identification of Electron Recoils
7. The CYGNO Apparatus
7.1. Detector Description
7.2. Background Simulation
7.3. Signal Simulation
8. Physics Performance
References

1. Bertone, G.; Hooper, D.; Silk, J. Particle dark matter: Evidence, candidates and constraints. *Phys. Rept.* **2005**, *405*, 279–390, [hep-ph/0404175]. doi:10.1016/j.physrep.2004.08.031.
2. Mayet, F.; others. A review of the discovery reach of directional Dark Matter detection. *Phys. Rept.* **2016**, *627*, 1–49, [arXiv:astro-ph.CO/1602.03781]. doi:10.1016/j.physrep.2016.02.007.
3. Zurek, K.M. Asymmetric Dark Matter: Theories, Signatures, and Constraints. *Phys. Rept.* **2014**, *537*, 91–121, [arXiv:hep-ph/1308.0338]. doi:10.1016/j.physrep.2013.12.001.

Table 1: Background rates. Copper costs (25 € /kg) assuming for CYGNO: 100 × 100 × 220 cm^3 internal shielding size; 0.583 m^3 for 5 cm; for LIME: 50 × 50 × 100 cm^3 internal shielding size; 0.162 m^3 for 5 cm, 0.406 m^3 for 10 cm, 1.188 m^3 for 20 cm; for 4×LIME: 90 × 90 × 200 cm^3 internal shielding size 1.040 m^3 for 10 cm

Detector Volume (m^3)	Water/Copper Thickness (cm)	Water Cost (k€)	Copper Cost (k€)	[1-20] keV cpy
1	250/5		150	1×10^2
1	200/5	370	150	5×10^2
1	100/5	70	150	2×10^5
1	85/5		150	1×10^6
1	50/5		150	8×10^6
0.05	-	-	-	3×10^8
0.05	50/5	20	40	5×10^5
0.05	50/10	20	95	5×10^4
0.05	100/5	25	40	3×10^4
0.05	110/10	25	95	2×10^3
0.05	50/20	20	270	1×10^3
0.40	90/10	50	250	2×10^4

4. Baracchini, E.; Derocco, W.; Dho, G. Discovering supernova-produced dark matter with directional detectors. *Phys. Rev. D* **2020**, *102*, 075036, [arXiv:hep-ph/2009.08836]. doi: 10.1103/PhysRevD.102.075036.
5. Seguinot, J.; Ypsilantis, T.; Zichichi, A. A High rate solar neutrino detector with energy determination. *Conf. Proc. C* **1992**, *920310*, 289–313.
6. Arpesella, C.; Broggini, C.; Cattadori, C. A possible gas for solar neutrino spectroscopy. *Astropart. Phys.* **1996**, *4*, 333–341. doi:10.1016/0927-6505(95)00051-8.
7. Vahsen, S.E.; others. CYGNUS: Feasibility of a nuclear recoil observatory with directional sensitivity to dark matter and neutrinos **2020**. [arXiv:physics.ins-det/2008.12587].
8. Marx, J.N.; Nygren, D.R. The Time Projection Chamber. *Phys. Today* **1978**, *31N10*, 46–53. doi: 10.1063/1.2994775.
9. Nygren, D.R. The Time Projection Chamber: A New 4 pi Detector for Charged Particles. *eConf* **1974**, *C740805*, 58.
10. Atwood, W.B.; others. Performance of the ALEPH time projection chamber. *Nucl. Instrum. Meth. A* **1991**, *306*, 446–458. doi:10.1016/0168-9002(91)90038-R.
11. Alme, J.; others. The ALICE TPC, a large 3-dimensional tracking device with fast readout for ultra-high multiplicity events. *Nucl. Instrum. Meth. A* **2010**, *622*, 316–367, [arXiv:physics.ins-det/1001.1950]. doi:10.1016/j.nima.2010.04.042.
12. Lippmann, C. Upgrade of the ALICE Time Projection Chamber **2014**.
13. Chardonnet, E. The DUNE dual-phase liquid argon TPC. *JINST* **2020**, *15*, C05064. doi: 10.1088/1748-0221/15/05/C05064.
14. Fraga, M.M.F.R.; Fraga, F.A.F.; Fetal, S.T.G.; Margato, L.M.S.; Ferreira-Marques, R.; Policarpo, A.J.P.L. The GEM scintillation in He CF_4, Ar CF_4, Ar TEA and Xe TEA mixtures. *Nucl. Instrum. Meth.* **2003**, *A504*, 88–92. doi:10.1016/S0168-9002(03)00758-7.
15. Margato, L.M.S.; Morozov, A.; Fraga, M.M.F.R.; Pereira, L.; Fraga, F.A.F. Effective decay time of CF_4 secondary scintillation. *JINST* **2013**, *8*, P07008. doi:10.1088/1748-0221/8/07/P07008.
16. Baracchini, E.; Benussi, L.; Bianco, S.; Capoccia, C.; Caponero, M.; Cavoto, G.; Cortez, A.; Costa, I.A.; Marco, E.D.; D'Imperio, G.; Dho, G.; Iacoangeli, F.; Maccarrone, G.; Marafini, M.; Mazzitelli, G.; Messina, A.; Orlandi, A.; Paoletti, E.; Passamonti, L.; Petrucci, F.; Piccolo, D.; Pierluigi, D.; Pinci, D.; Renga, F.; Rosatelli, F.; Russo, A.; Saviano, G.; Tomassini, S. First evidence of luminescence in a He/CF_4 gas mixture induced by non-ionizing electrons, 2020, [arXiv:physics.ins-det/2004.10493].
17. Dominik, W.; Zaganidis, N.; Astier, P.; Charpak, G.; Santiard, J.C.; Sauli, F.; Tribollet, E.; Geissbuhler, A.; Townsend, D. A GASEOUS DETECTOR FOR HIGH ACCURACY AUTORADIOGRAPHY OF RADIOACTIVE COMPOUNDS WITH OPTICAL READOUT OF

AVALANCHE POSITIONS. *Nucl. Instrum. Meth. A* **1989**, *278*, 779. doi:10.1016/0168-9002(89)91203-5.

18. Sauli, F. GEM: A new concept for electron amplification in gas detectors. *Nucl. Instrum. Meth. A* **1997**, *386*, 531–534. doi:10.1016/S0168-9002(96)01172-2.
19. Margato, L.M.S.; Fraga, F.A.F.; Fetal, S.T.G.; Fraga, M.M.F.R.; Balau, E.F.S.; Blanco, A.; Ferreira-Marques, R.; Policarpo, A.J.P.L. Performance of an optical readout GEM-based TPC. *Nucl. Instrum. Meth.* **2004**, *A535*, 231–235. doi:10.1016/j.nima.2004.07.126.
20. Marafini, M.; Patera, V.; Pinci, D.; Sarti, A.; Sciubba, A.; Spiriti, E. High granularity tracker based on a Triple-GEM optically read by a CMOS-based camera. *JINST* **2015**, *10*, P12010, [arXiv:physics.ins-det/1508.07143]. doi:10.1088/1748-0221/10/12/P12010.
21. Phan, N.S.; Lee, E.R.; Loomba, D. Imaging ^{55}Fe Electron Tracks in a GEM-based TPC Using a CCD Readout. *arXiv 1703.09883* **2017**, [arXiv:physics.ins-det/1703.09883].
22. Fraga, F.A.F.; Margato, L.M.S.; Fetal, S.T.; Fraga, M.M.F.R.; Ferreira-Marques, R.; Policarpo, A.J.P.L.; Guerard, B.; Oed, A.; Manzini, G.; van Vuure, T. CCD readout of GEM-based neutron detectors. *Nucl. Instrum. Meth. A* **2002**, *478*, 357–361. doi:10.1016/S0168-9002(01)01829-0.
23. Mavrokoridis, K.; Ball, F.; Carroll, J.; Lazos, M.; McCormick, K.J.; Smith, N.A.; Touramanis, C.; Walker, J. Optical Readout of a Two Phase Liquid Argon TPC using CCD Camera and THGEMs. *JINST* **2014**, *9*, P02006, [arXiv:physics.ins-det/1401.0525]. doi:10.1088/1748-0221/9/02/P02006.
24. Marafini, M.; Patera, V.; Pinci, D.; Sarti, A.; Sciubba, A.; Spiriti, E. ORANGE: A high sensitivity particle tracker based on optically read out GEM. *Nucl. Instrum. Meth.* **2017**, *A845*, 285–288. doi:10.1016/j.nima.2016.04.014.
25. Antochi, V.C.; Baracchini, E.; Cavoto, G.; Marco, E.D.; Marafini, M.; Mazzitelli, G.; Pinci, D.; Renga, F.; Tomassini, S.; Voena, C. Combined readout of a triple-GEM detector. *JINST* **2018**, *13*, P05001, [arXiv:physics.ins-det/1803.06860]. doi:10.1088/1748-0221/13/05/P05001.
26. Marafini, M.; Patera, V.; Pinci, D.; Sarti, A.; Sciubba, A.; Torchia, N.M. Study of the Performance of an Optically Readout Triple-GEM. *IEEE Transactions on Nuclear Science* **2018**, *65*, 604–608. doi:10.1109/TNS.2017.2778503.
27. Pinci, D.; Baracchini, E.; Cavoto, G.; Marco, E.D.; Marafini, M.; Mazzitelli, G.; Renga, F.; Tomassini, S.; Voena, C. High resolution TPC based on optically readout GEM. *Nuclear Instruments and Methods in Physics Research Section A: Accelerators, Spectrometers, Detectors and Associated Equipment* **2018**. doi:https://doi.org/10.1016/j.nima.2018.11.085.
28. Antochi, V.C.; Cavoto, G.; Costa, I.A.; Marco, E.D.; D'Imperio, G.; Iacoangeli, F.; Marafini, M.; Messina, A.; Pinci, D.; Renga, F.; Voena, C.; Baracchini, E.; Cortez, A.; Dho, G.; Benussi, L.; Bianco, S.; Capoccia, C.; Caponero, M.; Maccarrone, G.; Mazzitelli, G.; Orlandi, A.; Paoletti, E.; Passamonti, L.; Piccolo, D.; Pierluigi, D.; Rosatelli, F.; Russo, A.; Saviano, G.; Tomassini, S.; Nobrega, R.A.; Petrucci, F. A GEM-based Optically Readout Time Projection Chamber for charged particle tracking, 2020, [arXiv:physics.ins-det/2005.12272].
29. Costa, I.A.; Baracchini, E.; Bellini, F.; Benussi, L.; Bianco, S.; Caponero, M.; Cavoto, G.; D'Imperio, G.; Marco, E.D.; Maccarrone, G.; Marafini, M.; Mazzitelli, G.; Messina, A.; Petrucci, F.; Piccolo, D.; Pinci, D.; Renga, F.; Rosatelli, F.; Saviano, G.; Tomassini, S. Stability and detection performance of a GEM-based Optical Readout TPC with He/CF_4 gas mixtures. *Journal of Instrumentation* **2020**, *xx*, xxx. doi:yyy.
30. Campagnola, R. Study and optimization of the light-yield of a triple-GEM detector **2018**.
31. Veenhof, R. Garfield, a drift chamber simulation program. *Conf. Proc. C* **1993**, *9306149*, 66–71.
32. Veenhof, R. GARFIELD, recent developments. *Nucl. Instrum. Meth. A* **1998**, *419*, 726–730. doi:10.1016/S0168-9002(98)00851-1.
33. Agostinelli, S.; others. GEANT4: A Simulation toolkit. *Nucl. Instrum. Meth. A* **2003**, *506*, 250–303. doi:10.1016/S0168-9002(03)01368-8.
34. Costa, I.A.; Baracchini, E.; Bellini, F.; Benussi, L.; Bianco, S.; Caponero, M.; Cavoto, G.; D'Imperio, G.; Marco, E.D.; Maccarrone, G.; Marafini, M.; Mazzitelli, G.; Messina, A.; Petrucci, F.; Piccolo, D.; Pinci, D.; Renga, F.; Rosatelli, F.; Saviano, G.; Tomassini, S. Performance of optically readout GEM-based TPC with a 55Fe source. *Journal of Instrumentation* **2019**, *14*, P07011–P07011. doi:10.1088/1748-0221/14/07/p07011.
35. Antochi, V.; Baracchini, E.; Benussi, L.; Bianco, S.; Capoccia, C.; Caponero, M.; Cavoto, G.; Cortez, A.; Costa, I.; Di Marco, E.; et al.. Performance of an optically read out time projection chamber with ultra-relativistic electrons. *Nuclear Instruments and Methods in Physics Research Section A: Accelerators, Spectrometers, Detectors and Associated Equipment* **2021**, *999*, 165209, [arXiv:physics.ins-det/2005.12272v3]. doi:10.1016/j.nima.2021.165209.

36. B.Buonomo.; C.Di Giulio.; L.G.Foggetta.; P.Valente. A Hardware and Software Overview on the New BTF Transverse Profile Monitor. Proc. 5th Int. Beam Instrumentation Conf. (IBIC'16), Barcelona, Spain, 2016, pp. 818–821. doi:10.18429/JACoW-IBIC2016-WEPG73.
37. P.Valente.; B.Buonomo.; Di Giulio, C.; L.G.Foggetta. Frascati Beam-Test Facility (BTF) High Resolution Beam Spot Diagnostics. Proc. 5th Int. Beam Instrumentation Conf. (IBIC'16), Barcelona, Spain, 2016, pp. 222–225. doi:10.18429/JACoW-IBIC2016-MOPG65.
38. Blum, W.; Rolandi, L.; Riegler, W. *Particle detection with drift chambers*; Particle Acceleration and Detection, ISBN = 9783540766834, 2008. doi:10.1007/978-3-540-76684-1.
39. Baracchini, E.; others. A density-based clustering algorithm for the CYGNO data analysis. *JINST* **2020**, *15*, T12003, [arXiv:physics.ins-det/2007.01763]. doi:10.1088/1748-0221/15/12/T12003.
40. Ester, M.; Kriegel, H.P.; Sander, J.; Xu, X. A Density-based Algorithm for Discovering Clusters a Density-based Algorithm for Discovering Clusters in Large Spatial Databases with Noise. Proceedings of the Second International Conference on Knowledge Discovery and Data Mining. AAAI Press, 1996, KDD'96, pp. 226–231.
41. Baracchini, E.; others. Identification of low energy nuclear recoils in a gas TPC with optical readout **2020**. [arXiv:physics.ins-det/2007.12508]. doi:10.1088/1361-6501/abbd12.
42. Battat, J.B.R.; others. Reducing DRIFT Backgrounds with a Submicron Aluminized-Mylar Cathode. *Nucl. Instrum. Meth. A* **2015**, *794*, 33–46, [arXiv:physics.ins-det/1502.03535]. doi:10.1016/j.nima.2015.04.070.
43. Akl, M.A.; others. CMS Technical Design Report for the Muon Endcap GEM Upgrade **2015**.
44. Benussi, L.; Bianco, S.; Caponero, M.; Muhammad, S.; Passamonti, L.; Piccolo, D.; Pierluigi, D.; Raffone, G.; Russo, A.; Saviano, G. Fiber Bragg Grating sensors for deformation monitoring of GEM foils in HEP detectors. 6th IEEE International Workshop on Advances in Sensors and Interfaces, 2015, [arXiv:physics.ins-det/1512.08629]. doi:10.1109/IWASI.2015.7184954.
45. Riffard, Q.; others. MIMAC low energy electron-recoil discrimination measured with fast neutrons. *JINST* **2016**, *11*, P08011, [arXiv:astro-ph.IM/1602.01738]. doi:10.1088/1748-0221/11/08/P08011.
46. Phan, N.S.; Lauer, R.J.; Lee, E.R.; Loomba, D.; Matthews, J.A.J.; Miller, E.H. GEM-based TPC with CCD Imaging for Directional Dark Matter Detection. *Astropart. Phys.* **2016**, *84*, 82–96, [arXiv:physics.ins-det/1510.02170]. doi:10.1016/j.astropartphys.2016.08.006.
47. Baracchini, E.; others. First evidence of luminescence in a He/CF_4 gas mixture induced by non-ionizing electrons. *JINST* **2020**, *15*, P08018, [arXiv:physics.ins-det/2004.10493]. doi:10.1088/1748-0221/15/08/P08018.
48. Martoff, C.J.; Snowden-Ifft, D.P.; Ohnuki, T.; Spooner, N.; Lehner, M. Suppressing drift chamber diffusion without magnetic field. *Nucl. Instrum. Meth. A* **2000**, *440*, 355–359. doi:10.1016/S0168-9002(99)00955-9.
49. Ohnuki, T.; Snowden-Ifft, D.P.; Martoff, C.J. Measurement of carbon disulfide anion diffusion in a TPC. *Nucl. Instrum. Meth. A* **2001**, *463*, 142–148, [physics/0004006]. doi:10.1016/S0168-9002(01)00222-4.
50. Battat, J.B.R.; others. Low Threshold Results and Limits from the DRIFT Directional Dark Matter Detector. *Astropart. Phys.* **2017**, *91*, 65–74, [arXiv:astro-ph.IM/1701.00171]. doi:10.1016/j.astropartphys.2017.03.007.
51. Phan, N.S.; Lafler, R.; Lauer, R.J.; Lee, E.R.; Loomba, D.; Matthews, J.A.J.; Miller, E.H. The novel properties of SF_6 for directional dark matter experiments. *JINST* **2017**, *12*, P02012, [arXiv:physics.ins-det/1609.05249]. doi:10.1088/1748-0221/12/02/P02012.
52. Ikeda, T.; Shimada, T.; Ishiura, H.; Nakamura, K.D.; Nakamura, T.; Miuchi, K. Development of a negative ion micro TPC detector with SF_6 gas for the directional dark matter search. *JINST* **2020**, *15*, P07015, [arXiv:physics.ins-det/2004.09706]. doi:10.1088/1748-0221/15/07/P07015.
53. Lightfoot, P.K.; Spooner, N.J.C.; Lawson, T.B.; Aune, S.; Giomataris, I. First operation of bulk micromegas in low pressure negative ion drift gas mixtures for dark matter searches. *Astropart. Phys.* **2007**, *27*, 490–499. doi:10.1016/j.astropartphys.2007.02.003.
54. Baracchini, E.; Cavoto, G.; Mazzitelli, G.; Murtas, F.; Renga, F.; Tomassini, S. Negative Ion Time Projection Chamber operation with SF_6 at nearly atmospheric pressure. *JINST* **2018**, *13*, P04022, [arXiv:physics.ins-det/1710.01994]. doi:10.1088/1748-0221/13/04/P04022.
55. Nakamura, K.; others. Low pressure gas study for a direction-sensitive dark matter search experiment with MPGD. *JINST* **2012**, *7*, C02023. doi:10.1088/1748-0221/7/02/C02023.

56. Lewin, J.; Smith, P. Review of mathematics, numerical factors, and corrections for dark matter experiments based on elastic nuclear recoil. *Astroparticle Physics* **1996**, *6*, 87–112. doi: https://doi.org/10.1016/S0927-6505(96)00047-3.
57. Gondolo, P. Recoil momentum spectrum in directional dark matter detectors. *Physical Review D* **2002**, *66*, [arXiv:hep-ph/0209110v2]. doi:10.1103/physrevd.66.103513.
58. Baxter, D.; Bloch, I.M.; Bodnia, E.; Chen, X.; Conrad, J.; Gangi, P.D.; Dobson, J.E.Y.; Durnford, D.; Haselschwardt, S.J.; Kaboth, A.; Lang, R.F.; Lin, Q.; Lippincott, W.H.; Liu, J.; Manalaysay, A.; McCabe, C.; Mora, K.D.; Naim, D.; Neilson, R.; Olcina, I.; Piro, M.C.; Selvi, M.; von Krosigk, B.; Westerdale, S.; Yang, Y.; Zhou, N. Recommended conventions for reporting results from direct dark matter searches, 2021, [arXiv:hep-ex/2105.00599v1].
59. S. E. Vahsen, C. A. J. O'Hare, W.A.L.N.J.C.S.E.B. CYGNUS: Feasibility of a nuclear recoil observatory with directional sensitivity to dark matter and neutrinos. *arXiv:2008.12587*.
60. Aprile, E.; Aalbers, J.; Agostini, F.; Alfonsi, M.; Althueser, L.; Amaro, F.; Anthony, M.; Arneodo, F.; Baudis, L.; Bauermeister, B.; et al.. Dark Matter Search Results from a One Ton-Year Exposure of XENON1T. *Physical Review Letters* **2018**, *121*, [arXiv:astro-ph.CO/1805.12562v2]. doi:10.1103/physrevlett.121.111302.
61. Aprile, E.; Aalbers, J.; Agostini, F.; Alfonsi, M.; Althueser, L.; Amaro, F.; Antochi, V.; Angelino, E.; Arneodo, F.; Barge, D.; et al.. Light Dark Matter Search with Ionization Signals in XENON1T. *Physical Review Letters* **2019**, *123*, [arXiv:hep-ex/1907.11485v2]. doi:10.1103/physrevlett.123.251801.
62. Bœhm, C.; Cerdeño, D.; Machado, P.; Campo, A.O.D.; Reid, E. How high is the neutrino floor? *Journal of Cosmology and Astroparticle Physics* **2019**, *2019*, 043–043, [arXiv:hep-ph/1809.06385v4]. doi:10.1088/1475-7516/2019/01/043.
63. Agnes, P.; Albuquerque, I.; Alexander, T.; Alton, A.; Araujo, G.; Asner, D.; Ave, M.; Back, H.; Baldin, B.; Batignani, G.; et al.. Low-Mass Dark Matter Search with the DarkSide-50 Experiment. *Physical Review Letters* **2018**, *121*, [arXiv:astro-ph.HE/1802.06994v3]. doi:10.1103/physrevlett.121.081307.
64. Agnese, R.; Anderson, A.; Aralis, T.; Aramaki, T.; Arnquist, I.; Baker, W.; Balakishiyeva, D.; Barker, D.; Basu Thakur, R.; Bauer, D.; et al.. Low-mass dark matter search with CDMSlite. *Physical Review D* **2018**, *97*, [arXiv:astro-ph.CO/1707.01632v3]. doi:10.1103/physrevd.97.022002.
65. Mancuso, M.; others. Searches for Light Dark Matter with the CRESST-III Experiment. *J. Low Temp. Phys.* **2020**, *199*, 547–555. doi:10.1007/s10909-020-02343-3.
66. Savage, C.; Gelmini, G.; Gondolo, P.; Freese, K. Compatibility of DAMA/LIBRA dark matter detection with other searches. *Journal of Cosmology and Astroparticle Physics* **2009**, *2009*, 010–010, [arXiv:astro-ph/0808.3607v3]. doi:10.1088/1475-7516/2009/04/010.
67. Amole, C.; Ardid, M.; Arnquist, I.; Asner, D.; Baxter, D.; Behnke, E.; Bressler, M.; Broerman, B.; Cao, G.; Chen, C.; et al.. Dark matter search results from the complete exposure of the PICO-60 C3F8 bubble chamber. *Physical Review D* **2019**, *100*, [arXiv:astro-ph.CO/1902.04031v1]. doi:10.1103/physrevd.100.022001.
68. Savage, C.; Gondolo, P.; Freese, K. Can WIMP spin dependent couplings explain DAMA data, in light of null results from other experiments? *Physical Review D* **2004**, *70*, [arXiv:astro-ph/0408346v3]. doi:10.1103/physrevd.70.123513.
69. Battat, J.; Ezeribe, A.; Gauvreau, J.L.; Harton, J.; Lafler, R.; Law, E.; Lee, E.; Loomba, D.; Lumnah, A.; Miller, E.; et al.. Low threshold results and limits from the DRIFT directional dark matter detector. *Astroparticle Physics* **2017**, *91*, 65–74, [arXiv:astro-ph.IM/1701.00171v3]. doi:10.1016/j.astropartphys.2017.03.007.
70. Yakabe, R.; Nakamura, K.; Ikeda, T.; Ito, H.; Yamaguchi, Y.; Taishaku, R.; Nakazawa, M.; Ishiura, H.; Nakamura, T.; Shimada, T.; Tanimori, T.; Kubo, H.; Takada, A.; Sekiya, H.; Takeda, A.; Miuchi, K. First limits from a 3d-vector directional dark matter search with the NEWAGE-0.3b' detector, 2020, [arXiv:hep-ex/2005.05157].
71. Baracchini, E.; DeRocco, W.; Dho, G. Discovering supernova-produced dark matter with directional detectors. *Physical Review D* **2020**, *102*, [arXiv:hep-ph/2009.08836v1]. doi:10.1103/physrevd.102.075036.
72. DeRocco, W.; Graham, P.W.; Kasen, D.; Marques-Tavares, G.; Rajendran, S. Supernova signals of light dark matter. *Phys. Rev. D* **2019**, *100*, 075018, [arXiv:hep-ph/1905.09284]. doi:10.1103/PhysRevD.100.075018.

73. Billard, J.; Strigari, L.; Figueroa-Feliciano, E. Implication of neutrino backgrounds on the reach of next generation dark matter direct detection experiments. *Phys. Rev. D* **2014**, *89*, 023524, [arXiv:hep-ph/1307.5458]. doi:10.1103/PhysRevD.89.023524.
74. Bœhm, C.; Cerdeño, D.G.; Machado, P.A.N.; Olivares-Del Campo, A.; Perdomo, E.; Reid, E. How high is the neutrino floor? *JCAP* **2019**, *01*, 043, [arXiv:hep-ph/1809.06385]. doi: 10.1088/1475-7516/2019/01/043.
75. Soffitta, P.; Muleri, F.; Fabiani, S.; Costa, E.; Bellazzini, R.; Brez, A.; Minuti, M.; Pinchera, M.; Spandre, G. Measurement of the position resolution of the Gas Pixel Detector. *Nucl. Instrum. Meth. A* **2013**, *700*, 99–105, [arXiv:astro-ph.IM/1208.6330]. doi:10.1016/j.nima.2012.09.055.
76. Roszkowski, L.; Ruiz de Austri, R.; Silk, J.; Trotta, R. On prospects for dark matter indirect detection in the Constrained MSSM. *Physics Letters B* **2009**, *671*, 10–14, [0707.0622v2]. doi: https://doi.org/10.1016/j.physletb.2008.11.061.
77. Trotta, R.; de Austri, R.R.; Roszkowski, L. Prospects for direct dark matter detection in the constrained MSSM. *New Astronomy Reviews* **2007**, *51*, 316–320, [arXiv:astro-ph/0609126v1]. Francesco Melchiorri: Scientist, Pioneer, Mentor, doi:https://doi.org/10.1016/j.newar.2006.11.059.
78. Strege, C.; Trotta, R.; Bertone, G.; Peter, A.H.G.; Scott, P. Fundamental statistical limitations of future dark matter direct detection experiments. *Physical Review D* **2012**, *86*, [arXiv:hep-ph/1201.3631v2]. doi:10.1103/physrevd.86.023507.
79. Arina, C. Bayesian analysis of multiple direct detection experiments, 2014, [1310.5718].
80. Bringmann, T.; Conrad, J.; Cornell, J.M.; Dal, L.A.; Edsjö, J.; Farmer, B.; Kahlhoefer, F.; Kvellestad, A.; Putze, A.; et al.. DarkBit: a GAMBIT module for computing dark matter observables and likelihoods. *The European Physical Journal C* **2017**, *77*, [arXiv:hep-ph/1705.07920v2]. doi:10.1140/epjc/s10052-017-5155-4.
81. Liem, S.; Bertone, G.; Calore, F.; de Austri, R.R.; Tait, T.M.P.; Trotta, R.; Weniger, C. Effective field theory of dark matter: a global analysis. *Journal of High Energy Physics* **2016**, *2016*, [arXiv:hep-ph/1603.05994v1]. doi:10.1007/jhep09(2016)077.
82. Messina, A.; Nardecchia, M.; Piacentini, S. Annual modulations from secular variations: not relaxing DAMA? *Journal of Cosmology and Astroparticle Physics* **2020**, *2020*, 037–037, [arXiv:hep-ph/2003.03340v2]. doi:10.1088/1475-7516/2020/04/037.
83. di Cortona, G.G.; Messina, A.; Piacentini, S. Migdal effect and photon Bremsstrahlung: improving the sensitivity to light dark matter of liquid argon experiments. *Journal of High Energy Physics* **2020**, *2020*, [arXiv:hep-ph/2006.02453v2]. doi:10.1007/jhep11(2020)034.